International Journal of
Intelligent Engineering & Systems

http://www.inass.org/

# Optimal DG Integration in Power Distribution Systems Using Coronavirus Herd Immunity Optimizer

**Sarmad Ibrahim[1]*** **Shamam Alwash[1]**

[1]*Department of Electrical Engineering, University of Babylon, Babylon, Iraq*
* Corresponding author's Email: sarmad.ibrahim@uobabylon.edu.iq

**Abstract:** In this study, the problem of finding an optimal location and size of a distributed generator (DG) in distribution systems with considering operational distribution system constraints is proposed with the objective of maximizing DG hosting capacity (MDHC), reducing system loss, and improving voltage stability index (VSI). The proposed objective function is formulated as a multi-objective mixed-integer nonlinear optimization in order to solve it simultaneously. To solve this problem, the coronavirus herd immunity optimizer (CHIO), a bio-inspired metaheuristic optimization method, is herein proposed to simultaneously tackle a discrete and continuous DG integration problem in distribution systems. Extensive simulations on an IEEE 69-node system with different load levels and DG numbers are performed using MATLAB software to evaluate the efficacy of the proposed method. The simulation results demonstrate that the proposed method efficiently improves overall distribution system performance when compared to different DG numbers and load levels. Furthermore, the CHIO optimization method shows encouraging results and almost obtains the best results in all proposed cases when compared with well-known metaheuristic optimization methods such as genetic algorithm (GA), the hunger games search (HGS), the chaotic neural network algorithm (CNNA), and the water cycle algorithm (WCA). The CHIO can successfully offer a notable solution for the DG integration problem, and the obtained results, for example in case 1, revealed outperforming the CHIO compared to other methods in terms of the MDHC (i.e., 99.999 %), voltage profile improvement (i.e., the minimum voltage magnitude of 0.9696 p.u), VSI improvement (i.e., 29.16 %), and system loss reduction (i.e., 66.95 %) compared with the base case, respectively.

**Keywords:** Coronavirus herd immunity optimizer, DG integration, Maximize DG hosting capacity, Power loss reduction, Voltage stability index.

## 1. Introduction

Integration of renewable energy resources generally has several benefits to the power generation and distribution sectors due to their positive contribution to the environment and sustainable society. As a result of unbelievable exponential development in the renewable energy industry in terms of lower-cost power generation, most governments are speeding up the process of harnessing as maximum possible renewable energy sources mainly in response to climate change and energy scarcity. Furthermore, distributed renewable energy sources such as a distributed generator (DG) have emerged as an undeniable solution to various operational issues confronting a distribution system (DS) such as voltage profile fluctuating, high-energy system loss, and system reliability [1]. However, uncontrolled DG penetration can result in some operational challenges due to its intermittent nature. Voltage limit violations, thermal overloading challenges, failed protection systems, and deteriorating power quality are all included in the list of problems. Therefore, it is crucial to choose the right size and position of the DG required for integration without creating such problems [2]. Additionally, it is critical to ensure that the maximum DG injected into the DS does not go above what is permitted by the system's operating constraints. This procedure is essentially described as the maximum DG hosting capacity (MDHC) [3]. André Even originally suggested the notion of the hosting capacity (HC) in the context of distributed generating and defined it as the greatest number of DGs that may be incorporated into the DS before the system's performance deteriorates to unacceptable levels [4].

Many studies have recently investigated the evaluation of the integration of the DGs into DSs using various techniques with various objectives of DG integration.

Numerous strategies have been put forth to lower system losses and improve the DS's overall voltage profile using various techniques when the DG is present. For instance, an analytical method was proposed to assess the impact of optimal DG integration on the active and reactive losses in DS using particle swarm optimization [5]. The authors in [6] presented a comprehensive analysis of optimal DG location and size for a residential feeder intending to mainly improve loss reduction and the overall voltage profile. To demonstrate the superiority of the suggested strategy when compared to other methods, the authors of this research examined several cases employing various types of DGs. A new method was developed to integrate DGs into DSs to minimize the active power losses and enhance voltage stability margin [7]. The authors in [7] used the voltage stability margin index to find the best DG location and the optimum DG size is selected using MATLAB curve-fitting approximation. A new approach was presented to minimize the total system losses in DSs [8]. In this paper, the loss sensitivity factor is proposed for DG location and an intelligent water drop algorithm is used for optimal DG size. To lower system losses and improve voltage deviation, a hybrid metaheuristic technique using the salp swarm algorithm and whale optimization algorithm was suggested for solving the optimal DG location and size [9]. A modified moth flame optimization was proposed for solving the DG integration to improve the DS performance in terms of system losses, voltage deviation, and emission [10]. To minimize overall power losses and improve voltage and frequency profiles, the authors concentrated on determining the best placement and size for a photovoltaic distributed generation using particle swarm optimization and the genetic algorithm [11]. The DS's voltage stability index and network reconfiguration were both improved simultaneously by utilizing a modified water cycle algorithm in order to reduce system power losses while taking into account all operational restrictions [12].

Although the aforesaid methods have significantly improved the performance of DSs, they haven't taken into account MDHC in DSs and have instead simply integrated DG placement and size to achieve lower losses and optimize voltage profile.

Several researchers have concluded that distribution utilities can gain greater advantages from the optimal DG size and placement if MDHC, system loss, and voltage stability are all prioritized at the same time [13]. This is done in an effort to further enhance the DS's performance, not only in terms of improving voltage stability and reducing system loss but also in terms of MDHC. For instance, different researchers offered methods to simultaneously determine the best network reconfiguration and DG integration in order to maximize the MDHC and reduce system losses [14, 15]. Furthermore, some approaches were employed to maximize MDHC and improve overall system performance via well-known promising strategies using, mathematical, heuristic, and metaheuristic optimization techniques. These techniques have demonstrated their capacity to maximize the HC of distribution networks of various DG sizes.

For instance, in [16], A multi-objective bilevel optimization problem was formulated to maximize the total active losses reduction, the HC, and the annual total cost reduction for two real DSs. In this study, two case studies are conducted using DGs and a soft open point, including the deterministic and probabilistic case studies. In [17], a modified version of moth flame optimization was presented to enhance the DS capacity for hosting renewable energy by providing a novel bi-layer optimization model for DGs allocation in an active distribution network. In [18], to increase the DG hosting capacity of distribution networks, a new optimum static var compensator planning approach was presented. In this paper, a stochastic programming problem with two stages was used to formulate this problem.

Even if the simulation results from these techniques show a promising increase in the performance of the DS, it is still necessary to look for better overall performance.

The aforementioned studies proposed addressing the DG integration problem by focusing on either only the MDHC improvement or the MDHC and system loss reduction together with constrained voltage limits. In this study, the coronavirus herd immunity optimizer (CHIO) is used to suggest the best DG integration with the simultaneous goals of optimizing MDHC, minimizing system losses, and enhancing voltage stability index (VSI).

There are several cutting-edge optimizers inspired by nature or humans that may be utilized effectively to solve difficult OPs with high accuracy and quick convergence [19-21]. On the basis of an outstanding way of searching for a global solution, the CHIO is proposed in this article to provide an extra enhancement of the DS performance [22].

The CHIO optimization method is currently considered a state-of-the-art method and has been utilized effectively in many engineering disciplines to tackle challenging linear and nonlinear optimization problems (OPs) with remarkable accuracy and rapid convergence [23]. Several researchers have developed and used the CHIO to address optimization issues [24, 25]. For instance, a new fuzzy multi-criteria approach based on an improved CHIO is proposed to solve the reconfiguration problem in the DS with only binary variables [26]. However, nobody has taken into account both continuous and discrete variables simultaneously.

The primary contribution of this paper is to propose an efficient method to address the optimal DG integration problem into the DSs while taking into account all operational constraints. To overcome this problem, the CHIO is proposed, which addresses the non-linear multi-objective optimization problem while simultaneously dealing with discrete and continuous search spaces (e.g., DG allocation problem). Due to its high spreading rate, CHIO, which is based on the herd immunity (HI) concept, performs exceptionally well in navigating complicated search spaces. This helps the algorithm avoid becoming trapped on local solutions by exploring almost all feasible regions in search of the best solutions. Also, when it comes to balancing exploitation and exploration to find the optimal solution, CHIO is highly adept.

CHIO's goal is to find the best possible solution for the size and location of the DG that satisfies the MDHC, minimizes power loss, increases voltage stability, and keeps all operational constraints within tolerable limits. Various cases and comparisons are presented to further highlight and illustrate the effectiveness of the suggested method in terms of the MDHC, loss reduction, and VSI improvement while accounting for the existence of DGs in the DS.

The rest of this paper is structured as follows. The proposed CHIO is fully described in section 2. The formulation of the problem is shown in section 3. The case study is described in section 4. The numerical results and discussion are given in section 5. In section 6, the conclusion is described.

## 2. Proposed CHIO

This section first describes the structure of the suggested optimization approach for addressing problems before presenting how it works.

### 2.1 Inspiration

Viruses are tiny pathogens that can only multiply in an organism's live cells. They may spread physiologically and get amplified by multiplying hosts. In Wuhan, China, the corona-virus illness (COVID-19) was initially identified in December 2019. The disease's epidemic was reported by the world health organization. A novel strain of COVID-19 was discovered for the first time in Wuhan after several cases of pneumonia that seemed to have no known cause and the failure of the available vaccinations and therapies at that time.

Experts describe immunity as the body's natural resistance to infectious diseases or their toxins in both people and animals. Immunity may be inherent or learned. Individuals no longer get the sickness as a result. The HI is gained and the illness is stopped in its tracks when a significant portion of the population obtains this immunity [22].

### 2.2 Herd immunity

When a population has a sufficient number of individuals with an infection-specific immunity to successfully halt the spread of a disease, this is referred to as having HI [22].

HI mathematical modeling is the foundation of the CHIO. This algorithm is based on the idea that disease may be prevented in society by making the majority of the population amenable to vaccination. Because the immune population does not spread the disease, additional vulnerable members of the community are not affected. Fig. 1 depicts the concept of HI.

### 2.3 Population hierarchy

According to [22], HI is categorized into three groups based on the expanding population as shown in Fig. 2:

**a)** Susceptible persons: represents the greatest part of the population used to build the CHIO optimization structure, which can be defined as persons who are in direct touch with infected people.
**b)** Infected persons: it is considered the second biggest population which will increase if the social distance is not noticed until they are more secure or even pass away (i.e., confirmed cases).
**c)** Immune persons: persons whose numbers begin at zero and increase as the population increase. The pandemic eventually comes to an end after the vast majority of individuals are immune.

Received: July 27, 2022. Revised: August 16, 2022. 

### 2.4 Social distancing

In order to stop the spread of illnesses during viral pandemics, the idea of social distance is applied.

The idea of social distancing (SD) in the CHIO is focused on separating the present individual and the candidate from the group of individuals who may be susceptible, infected, or safe. The frequency of COVID-19 infection can be significantly decreased by the SD.

Fig. 3 illustrates how the disease's rate of transmission would slow due to social distance, which would eventually cause a pandemic to spring out. The disease's progress would be slowed and the pandemic's peak would be reached with fewer infected cases. As can be seen in Fig. 3, social isolation has reduced the incidence of the illness, which can even slow the spread of the illness and delay the peak of the epidemic [22].

### 2.5 Proposed CHIO procedure

This population-based meta-heuristic algorithm is based on the herb immunity approach which is modeled in the CHIO optimization algorithm. Following are the six main stages that make up the CHIO algorithm's structure [22]:

**Stage-1: Initialization**

This stage deals with the CHIO settings and the OP.

The OP is expressed in terms of the objective function as illustrated in Eq. (1):

$$\min_{\mathbf{x}} \quad f(\mathrm{x}) \qquad \mathrm{x} \in \{\mathrm{x}_{\min}, \mathrm{x}_{\max}\}$$

Subject to

$$\begin{aligned} g(\mathrm{x}) &= w_n \\ h(\mathrm{x}) &\geq z_n \end{aligned} \tag{1}$$

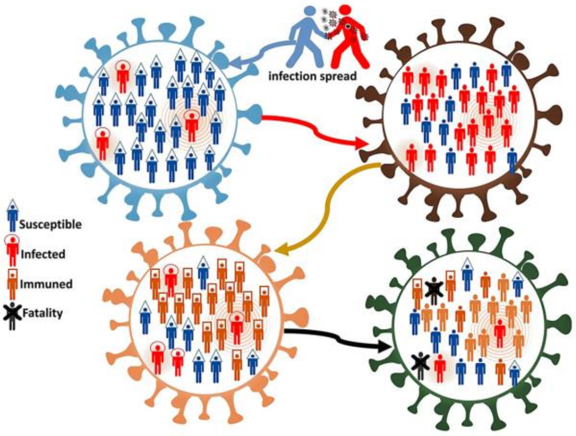


Figure. 1 An illustration of HI [22]

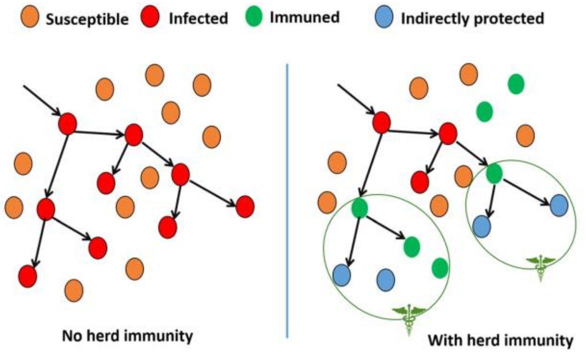


Figure. 2 Population hierarchy [22]

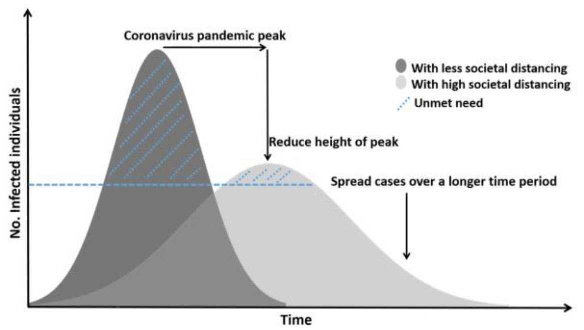


Figure. 3 Effect of SD on COVID-19 outbreaks [22]

Where **x** is a vector, $\mathrm{x} = (x_1, x_2, x_3, \dots \dots, x_{b)}$ , $b$ represents the total number of decision variables, $\mathrm{x}_{\min}$ and $\mathrm{x}_{\max}$ denote the minimum and maximum bounds of the decision variables, $g(\mathrm{x}) = w_n$ and $h(\mathrm{x}) \geq z_n$ represents the equality and inequality constraints.

The four algorithmic parameters of the CHIO algorithm are $C_0$ , which is the number of early instances of infection started by a single person (e.g., $C_0$ = 1), herd immunity size (HIS), the size of the population, $\mathrm{Max}_{Itr}$, the actual number of iterations, and n, which denotes the problem's dimensionality.

In addition, CHIO includes two control settings. The algorithm's operators are controlled by the BRr parameter, which stands for basic reproduction rate and is dependent on the virus's predominance. Furthermore, a control parameter called $\mathrm{Max}_{Age}$ specifies the average age of those that contract the virus, so once they reach $\mathrm{Max}_{Age}$, they either recover their health or pass away.

**Stage-2: Create the basic herd immunity population**

Generating a random starting population matrix is the first step in solving any OP, much like with any population-based meta-heuristic method. Therefore, the herd immunity population (HIP) with two-dimensional matrix $n \times HIS$ is generated as follows in Eq. (2) and (3):

 DOI: 10.22266/ijies2022.1231.13

$$HIP = \begin{bmatrix} x_1^1 & \cdots & x_n^1 \\ \vdots & \ddots & \vdots \\ x_1^{HIS} & \cdots & x_n^{HIS} \end{bmatrix} \quad (2)$$

Where $x_i^m$ is generated using Eq. (3).

$$x_i^m = \mathrm{x}_{\mathrm{min,i}} + (\mathrm{x}_{\mathrm{max,i}} - \mathrm{x}_{\mathrm{min,i}}) \times U(0,1) \quad (3)$$

Eq. (1) is used to determine the objective function (or immunity rate) for each case. Additionally, the status vector **S** is formed in all individuals of the HIP by either one (i.e., an infected individual) or zero (i.e., a susceptible person). Be aware that (S) has as many ones at random initiation as $C_0$.

**Stage-3: Evolution of herd immunity**

This stage is regarded as the main CHIO improvement loop. In this step, HIP is assessed using the following three rules to create a new HIP in which the individual gene, $x_i^m$, keeps the same or is affected by social distance. The three rules can be expressed in Eq. (4):

$$x_i^m(t+1) = \begin{cases} x_i^m(t), & r \geq \mathrm{BR}_r \\ C\left(x_i^m(t)\right), & r < \frac{1}{3} \times BR_r \\ N\left(x_i^m(t)\right), & r < \frac{2}{3} \times BR_r \\ R\left(x_i^m(t)\right), & \mathrm{r} < \mathrm{BR}_r \end{cases} \quad (4)$$

Where r is an integer chosen at random from [0, 1].

The first rule is infected case, which is ranged from 0 to $\frac{1}{3} \times BR_r$. The new gene is created by analyzing how the gene from the infected case varies from the current gene, but its value is reduced by SD, which can be determined using Eqs. (5) and (6) as follows:

$$x_i^m(t+1) = C\left(x_i^m(t)\right) \quad (5)$$

$$C\left(x_i^m(t)\right) = x_i^m(t) + r \times \left(x_i^m(t) - x_i^c(t)\right) \quad (6)$$

Where $x_i^c(t)$ is selected randomly from diseased person taken from infected case $\boldsymbol{x}^c$ based on the status vector **S**.

The second rule is the susceptible case. In this case, $x_i^m$will be modified based on SD calculating the difference between the current gene and a gene taken from any susceptible case $\boldsymbol{x}^b$ with considering $r$ within $\left[\frac{1}{3}BR_r, \frac{2}{3}BR_r\right]$, which is quantified by Eqs. (7) and (8) as follows:

$$x_i^m(t+1) = N\left(x_i^m(t)\right) \quad (7)$$

$$N\left(x_i^m(t)\right) = x_i^m(t) + r \times \left(x_i^m(t) - x_i^b(t)\right) \quad (8)$$

Where $x_i^b(t)$ is randomly chosen from the susceptible case according to the status vector S.

The last rule is the immune case, in this case, a new $x_i^m$ will be derived by SD considering $r$ within $\left[\frac{2}{3}BR_r, BR_r\right]$. The new gene is created by calculating the difference between the gene derived from the immune case $\boldsymbol{x}^v$ and the existing gene, which is quantified by Eqs. (9) and (10) as follows:

$$x_i^m(t+1) = R\left(x_i^m(t)\right) \quad (9)$$

$$R\left(x_i^m(t)\right) = x_i^m(t) + r \times \left(x_i^m(t) - x_i^v(t)\right) \quad (10)$$

Where $x_i^v(t)$ is randomly selected from the immune case depending on the status vector **S** such that

$$f(x^v) = \arg \min_{m \sim \{k|S_k=2\}} f(x^m) \quad (11)$$

**Stage -4: Update HIP**

In this stage, the HIP is updated by calculating the immunity rate $f(\boldsymbol{x}^m(t+1))$ for each created case $\boldsymbol{x}^m(t+1)$, and the generated case only replaces the present case $\boldsymbol{x}^m(t)$ if $f(\boldsymbol{x}^m(t+1)) < f(\boldsymbol{x}^m(t))$. Additionally, if the status vector, $S_m$ is equal to 1, the value of the age vector, $A_m$ is incremented to 1. The state vector, $S_m$ is modified, $\boldsymbol{x}^m$ for each iteration based on the herd immune criteria, which employs the following Eq. (12):

$$S_m = \begin{cases} 1 \quad f\left(\boldsymbol{x}^m(t+1)\right) < \frac{f(x)^m(t+1)}{\Delta f(x)} \wedge S_m = 0 \\ \quad \wedge \text{ is\_Corona}(\boldsymbol{x}^m(t+1)) \\ 2 \quad f\left(\boldsymbol{x}^m(t+1)\right) > \frac{f(x)^m(t+1)}{\Delta f(x)} \wedge S_m = 1 \end{cases} \quad (12)$$

If a new case has inherited a benefit from any infected cases, then is_Corona$(\boldsymbol{x}^m(t+1))$ is equal to 1, which is a binary value. Average population immune rates $\Delta f(\boldsymbol{x})$can be expressed in Eq. (13).

$$\Delta f(\boldsymbol{x}) = \frac{\sum_{i=1}^{HIS} f(x_i)}{HIS} \quad (13)$$

**Stage -5: Mortality cases**

For a specified iteration (i.e., $A_m \geq \mathrm{Max}_{Age}$), if the immunity rate $f\left(\boldsymbol{x}^m(t+1)\right)$ of the current infected person ($S_m = 1$) does not improve for the maximum repetition of the algorithm, then this process is considered as a lost person and then reproduced from scratch according to the following Eq. (14)

$$x_i^m(t+1) = \mathrm{x}_{\min,\mathrm{i}} + (\mathrm{x}_{\max,\mathrm{i}} - \mathrm{x}_{\min,\mathrm{i}}) \times U(0,1) \quad (14)$$

Additionally, $S_m$ and $A_m$ are both set to zero. Increasing the current population may help to avoid getting trapped in a local solution.

**Stage-6: Stopping condition**

The CHIO continues stages 3 through 6 until the terminating condition is met, which is generally determined by reaching the maximum number of iterations. In this case, the total number of vulnerable and immune cases dominates the population. Infected cases are also eradicated.

## 3. Problem formulation

The objective considered herein is to obtain the best possible solution for the MDHC, loss reduction, and VSI improvement based on the CHIO algorithm. This goal can be achieved by solving a complex multi-optimization problem with discrete and continuous variables (i.e., the DG location and size). In this work, the objective function (OF) will be calculated using a deterministic approach with constant DG generation with unity power factor and load consumption. The following is a description of the OF and constraints:

### 3.1 Objective function (OF)

This study combines the MDHC, total power loss index, and voltage stability index to create the suggested OF while simultaneously considering the best DG location and size injected into the DSs. The formulation of each component of the OF is as follows:

#### 3.1.1. Maximize DG hosting capacity (MDHC)

The MDHC, which is a percentage that cannot be higher than 100 %, is the ratio of all DG energy injected into the DSs to all connected loads. The MDHC is formulated in the following way represented in Eq. (15) [16]:

$$MDHC = 100.\frac{\sum_{i=1}^{N_{DG}} P_{DG,i}}{\sum_{j=1}^{N_L} P_{load,j}} \quad (15)$$

where $N_{DG}$ is the total number of DGs, $P_{DG,i}$ represents the DG generation injected at node $i$, $N_L$ is the total number of loads connected to the DS, $P_{load,j}$ represents the load connected at node $j$, $(i,j) \in N_{node}$, $N_{node}$ identifies the total number of nodes.

#### 3.1.2. Total active power loss

In general, the sum of the losses in all branches determines the total active loss, $P_{loss_T}$, dissipating in the DS, which is described in Eq. (16) [11]:

$$P_{loss_T} = \sum_{i=1}^{N_{br}} \frac{P_i^2+Q_i^2}{|V_i|^2} R_{i,j} \quad (16)$$

where $N_{br}$ denotes the total number of branches, active and reactive power drawn from node $i$ are represented by $P_i$ and $Q_i$, respectively, $V_i$ is a voltage at node $i$, $R_{ij}$ is branch's resistance that connects node $i$ and $j$, respectively.

#### 3.1.3. Voltage stability index (VSI)

The DS performance may be assessed using the VSI. The primary purpose of the VSI is to analyze how DSs behave with regard to voltage stability margin and identify any potential operating point instability of system nodes [27]. The following Eq. (17) is a representation of the VSI formula at node j:

$$\mathrm{VSI(j)} = |V_i|^2 - 4\big(P_j X_{ij} - Q_j R_{ij}\big)^2 - 4\big(P_j X_{ij} - Q_j R_{ij}\big)^2 |V_i|^2 \quad (17)$$

where active and reactive power load at node $j$ are indicated by $P_j$ and $Q_j$ represent, respectively, and $X_{ij}$ denotes reactance of the branch connecting node $i$ and $j$, respectively. Eq. (18) can be used to compute the minimal VSI.

$$\mathrm{VSI}_{min} = \min\,(\mathbf{VSI}) \quad (18)$$

#### 3.1.4. Operational constraints

The following operational constraints classify the stated equality and inequality constraints requirements of the OF that must be highlighted [16]:

**I.** All nodes in the DS must be kept within allowable bounds for inequality constraints expressed in Eq. (19):

$$V_{min} \le \left|\tilde{V}_i\right| \le V_{max}, \forall i \in \{1,2,\dots,N_{node}\} \quad (19)$$

Where $V_{min}$ and, $V_{max}$ indicates the lower and higher node voltage boundaries, respectively. The voltage magnitude constraints were determined to be 0.95 p.u. and 1.05 p.u. based on the ANSI standard

[25].

**II.** The active power balance constraint is a need for equality constraints to be satisfied and is defined in Eq. (20).

$$P_{loss_T} + P_{load_T} = P_{sub} + \sum_{i=1}^{N_{DG}} P_{DG,i} \quad (20)$$

where $P_{load_T}$ denotes the total load that is connected to the DS and $P_{sub}$ represents the total active power drawn from the main substation.

**III.** Another inequality constraint that is taken into account is the branch's current limitation, which is expressed by Eq. (21):

$$|I_b| \le I_b^{rated}, \forall b \in \{1,2, \dots, N_{br}\} \quad (21)$$

Where $I_b$ and $I_b^{rated}$ represent the current and maximum capacity of branch $b$.

**IV.** DG hosting capacity limits. The quantity of DG total active power output that may be injected into the DS should be constrained and not go over a specific threshold limit, which is mathematically defined using Eqs. (22) and (23):

$$0 \le \sum_{i=1}^{N_{DG}} P_{DG,i} \le P_{load_T} \quad (22)$$

or

$$MDHC \le 100\% \quad (23)$$

Finally, the objective function in this study is formulated by combining the MDHC, the active loss index, and the VSI. It is denoted by the following definitions using Eq. (24):

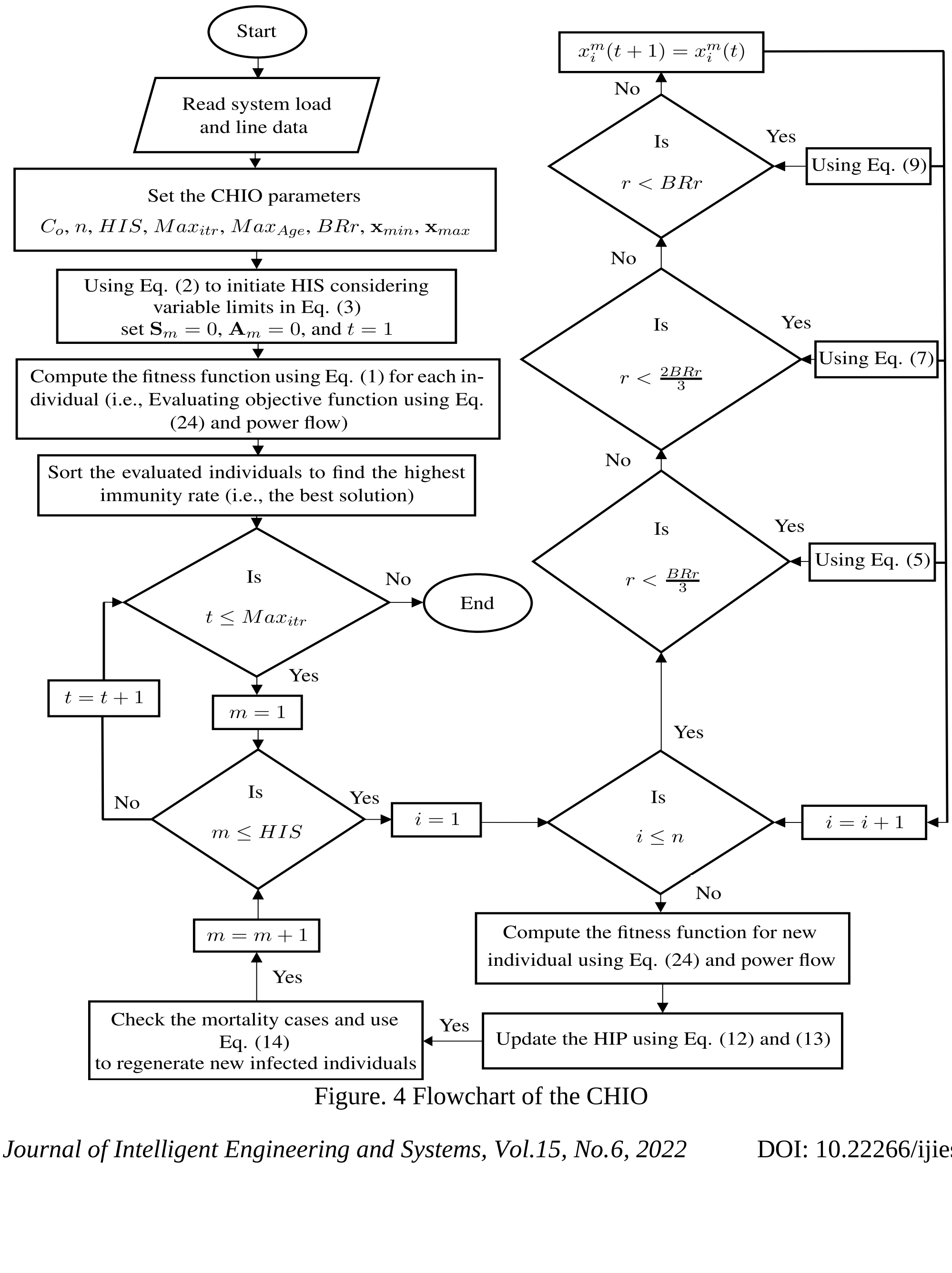

Figure. 4 Flowchart of the CHIO

$$OF = \min_{\mathbf{x}} \quad \left(w_1\left(1 - \frac{\sum_{i=1}^{N_{DG}} P_{DG,i}}{\sum_{j=1}^{N_L} P_{load,j}}\right) + w_2\left(\frac{P_{loss}}{P_{loss,0}}\right) + w_3(1 - \mathrm{VSI}_{min})\right) \quad (24)$$

where $\mathbf{x}$ is a row vector representing an initial candidate solution of the CHIO containing the DG locations and size, and weighted coefficients, $w_1$, $w_2$, and, $w_3$, are used to reduce a multi-objective OP into a single OP, $P_{loss,0}$ represents total active loss without DG injection. The objective function in Eq. (24) focuses primarily on the MDHC (i.e., $w_1$ = 0.5) and system losses (i.e., $w_2$ = 0.4), with a minor emphasis on voltage stability (i.e., $w_3$ = 0.1).

Fig. 4 highlights the primary structure of the proposed CHIO employed in this paper.

## 4. Case study

The test system used in this paper is an IEEE 69-node radial DS to test the performance of the suggested technique as shown in Fig. 5. The total load is 3.8022 MW and 2.6941 MVAr, and the nominal voltage is set to 12.66 kV (or 1 p.u.). This DS contains 69 nodes and 73 branches. It generally has 5 opened tie switches, which are shown by dotted lines, and 68 closed sectionalizing switches, which are shown by solid lines [29].

Using the IEEE 69-node radial DS, the efficacy of the suggested method will be evaluated, and four different cases with different numbers of DGs are run to maximize MDHC, reduce losses, and improve VSI using the CHIO while taking into account all operational limits. In addition to the base case, these cases are categorized as follows:

***Base case***: It is the case without considering the DG installation.
***Case 1***: It is a nominal load, which is 100 % of the system load.
***Case 2***: It is a heavy load in which active and reactive power loads are decreased by 50 % of the system load.
***Case 3***: It is a light load in which active and reactive power loads are increased by 50 % of the system load.

The superiority of the proposed method is verified by solving the same proposed problem using well-known meta-heuristic algorithms. Only case 1 is used for comparison between the CHIO and others. These compared algorithms are briefly described as follows:

The genetic algorithm (GA) is a genetic and natural selection-based evolutionary algorithm that draws its inspiration from the thought processes that underlie biological evolution [29]. The hunger games search (HGS) is a metaheuristic algorithm based on the behaviors and actions taken by animals in their pursuit of food when they are driven by hunger [30]. The chaotic neural network algorithm (CNNA) is a metaheuristic algorithm that uses randomization and artificial neural networks to tackle optimization issues. Artificial neural networks and human nerve systems served as inspiration for this method [31]. The water cycle algorithm (WCA) is a meta-heuristic technique that was developed after studying how water moves naturally [32].

A power flow approach [33] is utilized in this study to assess the viability of proposed solutions. Different numbers of DGs are recommended for installation in the DS. The DG size restrictions are set to be between 0 and 4 MVA.

## 5. Numerical results and discussions

Table 1 shows the simulations of the four cases discussed above. The basic case, as shown in Table 1, is the case without DG injection in the test system. This is the worst case according to loss reduction, voltage magnitude violation, and minimal VSI. Table 1 also includes case 1. In this case, three DGs are sequentially injected. It can be observed that the number of DGs can give a positive impact on the system performance. As shown in Table 1, one DG is optimally selected by CHIO with optimal location and size in which the MDHC is significantly improved by 99.999 %, the system loss reduction improved to 23.08 %, the minimum voltage magnitude within permissible limits, and the minimum VSI is improved by 22.58 %. It can be also observed that the system loss has improved slightly because the CHIO is limited by one DG injection. That means the search space is extremely restricted by one location. As a result, the CHIO selected the optimal DG position and size that does not violate the system operating limits while optimizing the proposed OF.

In the case of two DGs for case 1, the CHIO has greater flexibility to improve the overall system performance and it is clearly seen from the results in Table 1. In this case, when compared to the base case, the MDHC, system loss reduction, and minimum VSI are greatly improved by 99.994 %, 62.76 %, and 28.39 %, respectively. Furthermore, the minimum voltage magnitude is within permitted limits. In the case of three DGs, the CHIO selected three DGs to be injected at optimal locations and sizes as shown in Fig. 5. From Table 1, as compared with the base case, MDHC is significantly improved by 99.999 %, the system loss reduction improved to 66.95 %, and the minimum voltage magnitude is improved to above acceptable limits, while minimum VSI has a modest

Received: July 27, 2022. Revised: August 16, 2022. 

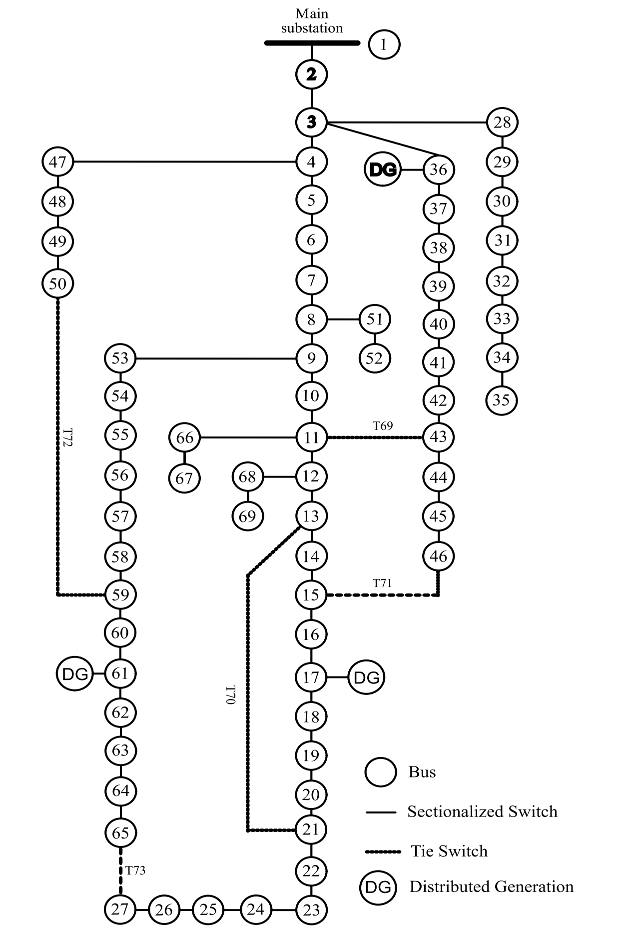


Figure. 5 The optimal DG location for modified IEEE 69-node radial DS (i.e., case 1)

improvement, which is nearly 29.22 %. This is expected because the proposed method mainly focuses on the MDHC and loss reduction with less emphasis on the VSI.

Case 2 is also included in Table 1. In this case, the load system is increased by 1.5 percent (i.e., the total system load is 5.7033 MW and 4.041 MVAr) to show the proposed method's efficacy and whether it can improve the system performance or not when the system load is increased. From Table 1, the CHIO selected one DG with the maximum DG capacity (i.e., $S_{DGmax}$ = 4 MVA) and optimal location (i.e., node 61) to improve the overall system performance.

In the case of one DG for case 2, the MDHC is enhanced but has less improvement than in case 1. This is understandable since the active power of the load system has increased by 150 percent when compared to case 1, and the $S_{DGmax}$ is smaller than the active power of the load system. Additionally, in comparison to the base case, the system loss reduction improved to 57.947 %, the minimum voltage magnitude is within acceptable limits, whereas the minimum VSI is significantly improved to 55.586 % due to the increase in the load system. Additionally, Table 1 demonstrates that the use of

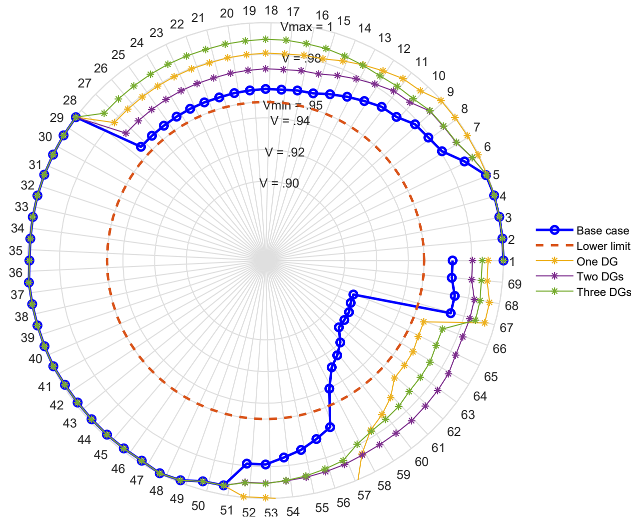


Figure. 6 Voltage profile for case 1

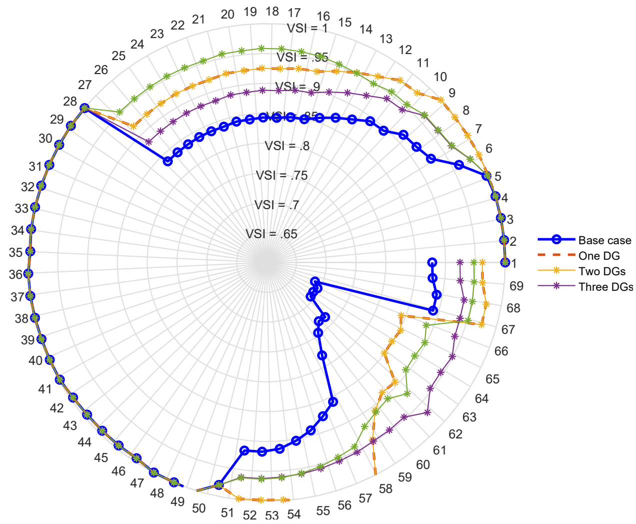


Figure. 7 VSI profile for case 1

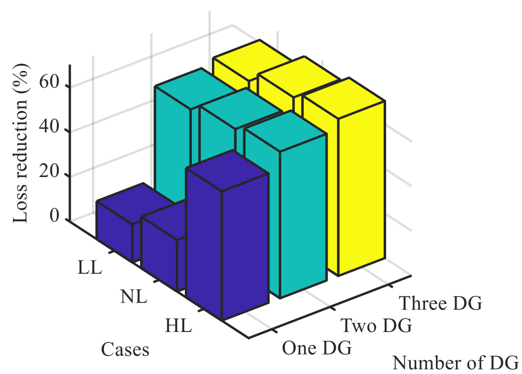


Figure. 8 The influence of DG size and location on loss reduction percentage for all cases

two and three DGs successfully enhances the test system's overall performance in case 2 when compared to the base case and one DG case. For instance, in the case of three DGs, the MDHC, system loss reduction, and the minimum VSI are greatly enhanced by 99.82 %, 70.377 %, and 59.77 %,

Received: July 27, 2022. Revised: August 16, 2022. 

Table 1. Numerical results of the proposed CHIO with different load levels

| No. of DG | DG size (MW) | DG location | MDHC (%) | Power loss (kW) | Loss reduction (%) | Vmax/Vmin (p.u) | Min VSI (p.u) |
|---|---|---|---|---|---|---|---|
| | **Case1 (Nominal Load 100%, $S_{DGmax}$ = 4 MVA)** | | | | | | |
| Base case | ----- | ------ | ------ | 224.50 | 0.00 | 1/ 0.9094 | 0.6872 |
| 1 | 3.8018 | 56 | 99.999 | 172.70 | 23.08 | 1/ 0.9569 | 0.8424 |
| 2 | 1.8019, 2.0000 | 40, 61 | 99.999 | 83.60 | 62.76 | 1/0.9691 | 0.8823 |
| 3 | 0.5299, 1.7607, 1.5111 | 17, 36, 61 | 99.999 | 74.20 | 66.95 | 1/0.9696 | 0.8880 |
| | **Case2 (Heavy Load 150%, $S_{DGmax}$ = 4 MVA)** | | | | | | |
| Base case | ----- | ------ | ------ | 558.80 | 0.00 | 1/ 0.8563 | 0.5424 |
| 1 | 4.000 | 61 | 70.14 | 234.99 | 57.947 | 1/0.9584 | 0.8439 |
| 2 | 2.928, 2.772 | 47, 61 | 99.95 | 191.82 | 65.672 | 1/0.9515 | 0.8497 |
| 3 | 0.903, 2.255, 2.534 | 16, 40, 61 | 99.82 | 165.53 | 70.377 | 1/0.9632 | 0.8666 |
| | **Case3 (Light Load 50%, $S_{DGmax}$ = 4 MVA)** | | | | | | |
| Base case | ----- | ------ | ------ | 51.5 | 0.00 | 1/ 0.9568 | 0.8398 |
| 1 | 1.9003 | 7 | 99.960 | 42.72 | 17.04 | 1/ 0.9663 | 0.8739 |
| 2 | 1.131, 0.767 | 28, 62 | 99.840 | 21.35 | 58.54 | 1/ 0.9835 | 0.9357 |
| 3 | 0.363, 0.917,0.611 | 12, 47, 61 | 99.480 | 19.96 | 61.24 | 1/ 0.9810 | 0.9272 |

Table 2. Numerical results of the proposed CHIO for case 1 in a comparison with other methods

| No. of DG | | DG size (MW) | DG location | MDHC (%) | Loss reduction (%) | Vmax/Vmin (p.u) | Min VSI (p.u) |
|---|---|---|---|---|---|---|---|
| Base case | | ----- | ------ | ------ | ---- | 1/ 0.9094 | 0.6872 |
| 1 | GA | 3.800 | 56 | 99.942 | 23.10 | 1/0.9569 | 0.8424 |
| | HGS | 3.8018 | 56 | 99.999 | 23.08 | 1/0.9570 | 0.8424 |
| | CNNA | 3.8018 | 56 | 99.999 | 23.08 | 1/0.9569 | 0.8424 |
| | WCA | 3.8018 | 56 | 99.999 | 23.08 | 1/0.9569 | 0.8424 |
| | CHIO | 3.8018 | 56 | 99.999 | 23.08 | 1/ 0.9569 | 0.8424 |
| 2 | GA | 2.072, 1.708 | 36, 61 | 99.416 | 62.54 | 1/0.9674 | 0.8760 |
| | HGS | 2.161, 1.641 | 4, 61 | 99.999 | 62.18 | 1/0.9670 | 0.8746 |
| | CNNA | 2.140, 1.662 | 4, 61 | 99.999 | 62.33 | 1/0.9672 | 0.8751 |
| | WCA | 2.057, 1.745 | 47, 61 | 99.999 | 62.76 | 1/0.9676 | 0.8768 |
| | CHIO | 1.8019, 2.000 | 40, 61 | 99.999 | 62.76 | 1/0.9691 | 0.8823 |
| 3 | GA | 0.424, 1.644, 1.732 | 12, 28, 61 | 99.942 | 66.59 | 1/0.9748 | 0.9030 |
| | HGS | 1.104, 1.293, 1.405 | 3, 11, 61 | 99.999 | 65.55 | 1/0.9703 | 0.8903 |
| | CNNA | 1.046, 1.3245, 1.431 | 10, 49, 61 | 99.999 | 66.20 | 1/0.9697 | 0.8880 |
| | WCA | 1.506, 0.877, 1.419 | 2, 12, 61 | 99.999 | 66.24 | 1/0.9684 | 0.8830 |
| | CHIO | 0.529, 1.761, 1.511 | 17, 36, 61 | 99.999 | 66.95 | 1/0.9696 | 0.8880 |

respectively, compared with the base case. Table 1 further shows that in all cases, the CHIO is successful in optimizing DG position and size, with all system nodes remaining within the allowable limits.

Finally, Table 1 depicts case 3. In this case, the load system is reduced by half (i.e., the total load is 1.9011 MW and 1.3470 MVAr) to demonstrate the usefulness of the suggested technique. As indicated in Table 1 for case 3, the base case is considered as a moderate case in terms of system loss, voltage magnitude violation, and minimum VSI due to load system reduction. Nevertheless, the CHIO is successful in optimizing DG position and size in cases of injection one, two, and three DGs. In the case of three DG injections, for example, the CHIO chose three DGs to be injected in appropriate locations and sizes. From Table 1, as compared with the base case, MDHC is significantly improved to 99.480 %, the system loss reduction improved to 61.24 %, and the minimum voltage magnitude is significantly improved to above acceptable limits, while minimum VSI is improved by 10.40 %.

Figs. 6 and 7 compare the voltage profile and VSI for case 1, including the basic case. Fig. 6 illustrates that the CHIO successfully selected the optimal DG locations and sizes, with the voltage magnitude at each node in the test system being within acceptable limits. Furthermore, Fig. 7 shows the VSI improvement for all system nodes compared with the base case.

As an example of the suggested CHIO, Fig. 8 shows the influence of DGs with varied penetration levels on the loss reduction percentage for all cases. The presence of DGs with high penetration levels boosts the magnitude of the voltage. As a result, as illustrated in Fig. 8, the system loss reduction will be greatly improved.

Table 2 compares the proposed method and the existing ones discussed in section 4 just for case 1 using the same metrics in Table 1 except a power loss metric. As seen in Table 2 in the case of one DG, all comprising methods get the same results except GA. This is expected due to limited search space that is constrained by one control variable (i.e., DG location and size). When the search space is enlarged by increasing the control variables represented by DGs, the capacity of the proposed approach and other methods to discover superior results becomes apparent. According to Table 2, the CHIO and WCA methods are similar in terms of maximizing MHDC and outperforming other methods in terms of loss reduction and minimal VSI improvement when two DGs are used as variable controls. This is expected because both CHIO and WCA have a comparable ability to investigate almost all feasible regions in search space due to continuously changing the positions of candidate solutions to avoid becoming trapped in a local solution. However, the CHIO surpasses the WCA in terms of increasing the minimal VSI.

In the case of three DGs, as shown in Table 2, the CHIO shows the best performance improvement, especially in reducing the system losses.

This is expected because CHIO has a high spreading rate and excels at navigating complex search spaces because it is built on the HI concept.

## 6. Conclusion

An integrated approach, expressed as a mixed-integer and non-linear optimization problem, is proposed to maximize DG hosting capacity (MDHC), decrease system loss, and increase voltage stability index (VSI) in distribution networks while restraining undesirable voltage magnitudes. The integrated technique is based on simultaneously determining an appropriate DG placement and size, which is solved using a coronavirus herd immunity optimizer (CHIO). The proposed method's performance is assessed using the IEEE 69-node radial DS at varying load levels and DG numbers, and it is compared to other existing approaches. Four cases are considered: base case, nominal load, heavy load, and light load. The results demonstrate the efficacy of the suggested method in achieving the stated goal when compared to well-known metaheuristic optimization methods. In each of these cases, the CHIO is capable of increasing MDHC by 70.14–99.99 %, decreasing DS losses by 17.04–70.37 %, increasing minimum VSI by 10.40–59.77 %, and maintaining acceptable voltage magnitudes.

## Conflicts of interest

The authors declare no conflict of interest.

## Author contributions

The manuscript has been prepared by the 1st author while the review and editing have been performed by the 1st author and 2nd author.

## References

[1] S. E. Razavi, E. Rahimi, and M. S. Javaid, "Impact of distributed generation on protection and voltage regulation of distribution systems: A review", *Renewable and Sustainable Energy Reviews*, Vol.105, pp.157–167, 2019.

[2] Prashant, A. S. Siddiqui, M. Sarwar, A. Althobaiti, and S. S. M. Ghoneim, "Optimal Location and Sizing of Distributed Generators in Power System Network with Power Quality Enhancement Using Fuzzy Logic Controlled D-STATCOM", *Sustainability*, Vol. 14, pp. 157–167, 2022.

[3] S. M. Ismael, S. H. E. A. Aleem, A. Y. Abdelaziz, and A. F. Zobaa, "State-of-the-art of hosting capacity in modern power systems with distributed generation", *Renewable Energy*, Vol. 130, pp. 1002–1020, 2019.

[4] M. H. J. Bollen and S. K. Rönnberg, "Hosting Capacity of the Power Grid for Renewable Electricity Production and New Large Consumption Equipment", *Energies*, Vol. 10, No. 9, pp. 1–28, 2017.

[5] A. P. Adeagbo, F. K. Ariyo, K. A. Makinde, S. A. Salimon, O. B. Adewuyi, and O. K. Akinde, "Integration of Solar Photovoltaic Distributed Generators in Distribution Networks Based on Site's Condition", *Solar*, Vol. 2, pp. 52–63, 2022.

[6] M. F. Aman, X. C. Ren, Tareen, W. U. K., K. Tareen, M. A. Khan, M. R. Anjum, A. M. Hashmi, H. Ali, I. Bari, J. Khan, and S. Ahmad, "Optimal Siting of Distributed Generation Unit in Power Distribution System considering Voltage Profile and Power Losses", *Hindawi*, Vol. 2022, pp. 594–605, 2022.

[7] S. Essallah, A. Khedher, and A. Bouallegue, "Integration of distributed generation in electrical grid: Optimal placement and sizing

under different load conditions", *Computers & Electrical Engineering*, Vol. 79, No. 2, pp. 854–867, 2019.

[8] D. R. Prabha, T. Jayabarathi, R. Umamageswari, and S. Saranya, "Optimal location and sizing of distributed generation unit using intelligent water drop algorithm", *Sustainable Energy Technologies and Assessments*, Vol. 11, pp. 106–113, 2015.

[9] K. M. S. Alzaidi, O. Bayatand, and O. N. Uçan, "Multiple DGs for Reducing Total Power Losses in Radial Distribution Systems Using Hybrid WOA-SSA Algorithm", *International Journal of Photoenergy, Hindawi*, Vol. 2019, pp. 1–20, 2019.

[10] E. E. Elattar and S. K. Elsayed, "Optimal Location and Sizing of Distributed Generators Based on Renewable Energy Sources Using Modified Moth Flame Optimization Technique", *IEEE Access*, Vol. 8, No. 6, pp. 109625–109638, 2020.

[11] I. Khenissi, R. Sellami, M. A. Fakhfakh, and R. Nejiet, "Power Loss Minimization Using Optimal Placement and Sizing of Photovoltaic Distributed Generation Under Daily Load Consumption Profile with PSO and GA Algorithms", *Journal of Control, Automation and Electrical Systems*, Vol. 32, pp. 1317–1331, 2021.

[12] S. Ibrahim, S. Alwash, and A. Aldhahab, "Optimal Network Reconfiguration and DG Integration in Power Distribution Systems Using Enhanced Water Cycle Algorithm", *International Journal of Intelligent Engineering and Systems*, Vol. 13, No. 1, pp. 379–389, 2020, doi: 10.22266/ijies2020.0229.35.

[13] B. Azibek, A. Abukhan, H. S. V. S. K. Nunna, B. Mukatov, S. Kamalasadan, and S. Doolla, "Hosting Capacity Enhancement in Low Voltage Distribution Networks: Challenges and Solutions", In: *Proc. of IEEE International Conference on Power Electronics, Smart Grid and Renewable Energy*, pp. 1–6, 2020.

[14] R. Čađenović and D.Jakus, "Maximization of Distribution Network Hosting Capacity through Optimal Grid Reconfiguration and Distributed Generation Capacity Allocation/Control", *Energies*, Vol. 13, pp. 1–17, 2020.

[15] Z. M. Ali, I. M. Diaaeldin, S. H. E. A. Aleem, A. E. Rafei, A. Y. Abdelaziz, and F. Jurado, "Scenario-Based Network Reconfiguration and Renewable Energy Resources Integration in Large-Scale Distribution Systems Considering Parameters Uncertainty", *Mathematics*, Vol. 9, No. 6, pp. 1–32, 2021.

[16] I. M. Diaaeldin, S. H. E. A. Aleem, A. E. Rafei, A. Y. Abdelaziz, and A. F. Zobaa, "Enhancement of Hosting Capacity with Soft Open Points and Distribution System Reconfiguration: Multi-Objective Bilevel Stochastic Optimization", *Energies*, Vol. 13, pp. 1–20, 2020.

[17] P. Singh and S. K. Bishnoi, "Modified Moth-Flame optimization for strategic integration of fuel cell in renewable active distribution network", *Electric Power Systems Research*, Vol. 197, pp. 1–18, 2021.

[18] X. Xu, J. Li, Z. Xu, J. Zhao, and C. S. Lai, "Enhancing photovoltaic hosting capacity—A stochastic approach to optimal planning of static var compensator devices in distribution networks", *Applied Energy*, Vol. 238, pp. 952–962, 2019.

[19] P. D. Kusuma and M. Kallista, "Stochastic Komodo Algorithm", *International Journal of Intelligent Engineering and Systems*, Vol. 15, No. 4, pp. 156–166, 2022, doi: 10.22266/ijies2022.0831.15.

[20] F. A. Zeidabadi and M. Dehghani, "POA: Puzzle Optimization Algorithm", *International Journal of Intelligent Engineering and Systems*, Vol. 15, No. 1, pp. 273–281, 2022, doi: 10.22266/ijies2022.0228.25.

[21] S. A. Doumariand, H. Givi, M. Dehghani, and O. P. Malik "Ring Toss Game-Based Optimization Algorithm for Solving Various Optimization Problems", *International Journal of Intelligent Engineering and Systems*, Vol. 14, No. 3, pp. 545–554, 2021, doi: 10.22266/ijies2021.0630.46.

[22] M. A. A. Betar, Z. A. A. Alyasseri, M. A. Awadallah, and I. A. Doush, "Coronavirus herd immunity optimizer (CHIO)", *Neural Computer & Application*, Vol. 33, pp. 5011–5042, 2021.

[23] S. Amini, S. Ghasemi, H. Golpira, and A. A. Moghaddam, "Coronavirus Herd Immunity Optimizer (CHIO) for Transmission Expansion Planning", In: *Proc. of IEEE International Conf. on Environment and Electrical Engineering and 2021 IEEE Industrial and Commercial Power Systems Europe*, Bari, Italy, pp. 1–6, 2021.

[24] S. N. Makhadmeh, M. A. A. Betar, M. A. Awadallah, A. K. Abasi, Z. A. A. Alyasseri, I. A. Doush, O. A. Alomari, R. Damaševičius, A. Zajančkauskas, and M. A. Mohammed, "A Modified Coronavirus Herd Immunity Optimizer for the Power Scheduling Problem", *Mathematics*, Vol. 10, pp. 1–29, 2022.

[25] C. Kumar, D. M. Mary, and T. Gunasekar, "MOCHIO: a novel Multi-Objective

Coronavirus Herd Immunity Optimization algorithm for solving brushless direct current wheel motor design optimization problem", A*utomatika*, Vol. 63, No. 1, pp. 149–170, 2022.
[26] A. Naderipour, A. Abdullah, M. H. Marzbali, and S. A. Nowdeh, "An improved corona-virus herd immunity optimizer algorithm for network reconfiguration based on fuzzy multi-criteria approach", *Expert Systems with Applications*, Vol. 187, pp. 1–21, 2022.
[27] M. Chakravorty and D. Das, "Voltage Stability Analysis of Radial Distribution Networks", *International Journal of Electrical Power & Energy Systems*, Vol. 23, No. 2, pp. 129-135, 2001.
[28] "American National Standard for Electric Power Systems and Equipment Voltage Ratings (60) Hertz", *The American National Standards Institute (ANSI)*, NSI, C84. pp. 1-1995, 1996.
[29] N. C. Sahoo and K. Prasad, "A Fuzzy Genetic Approach for Network Reconfiguration to Enhance Voltage Stability in Radial Distribution Systems", *Energy Conversion and Management*, Vol. 47, No. 18, pp. 3288–3306, 2006.
[30] Y. Yang, H. Chen, A. A. Heidari, and A. H. Gandomi, "Hunger games search: Visions, conception, implementation, deep analysis, perspectives, and towards performance shifts", *Expert Systems with Applications*, Vol. 177, pp. 1–34, 2021.
[31] Y. Zhang, "Chaotic neural network algorithm with competitive learning for global optimization", *Knowledge-Based Systems*, Vol. 231, pp. 1–16, 2021.
[32] A. Sadollah, H. Eskandar, and J. H. Kim, "Water Cycle Algorithm for Solving Constrained Multi-Objective Optimization Problems", *Applied Soft Computing*, Vol. 27, No. 4, pp. 279–298, 2015.
[33] W. H. Kersting, "Distribution System Modeling and Analysis", *CRC Press*, Boca Raton, N.Y, Vol. 3, 2015.